Korean J. Chem. Eng., 39(2), 423-430 (2022)
DOI: 10.1007/s11814-021-0921-2

pISSN: 0256-1115
eISSN: 1975-7220

Optimization of synergistic green emulsion liquid membrane stability for enhancement of silver recovery from aqueous solution

Norela Jusoh[*,], Norasikin Othman[*,**,†], Raja Norimie Raja Sulaiman[*,**], Norul Fatiha Mohamed Noah[*], and Muhammad Abbas Ahmad Zaini[*,**]**

*School of Chemical and Energy Engineering, Faculty of Engineering, Universiti Teknologi Malaysia, 81310 UTM Johor Bahru, Johor, Malaysia
**Centre of Lipids Engineering and Applied Research (CLEAR), Ibnu Sina Institute for Scientific and Industrial Research (ISI-SIR), Universiti Teknologi Malaysia, 81310 UTM Johor Bahru, Johor, Malaysia
(*Received 21 April 2021 • Revised 21 July 2021 • Accepted 8 August 2021*)

Abstract−The emulsion liquid membrane (ELM) process for silver recovery containing synergistic Cyanex 302/Cyanex 272 carriers, palm oil as a diluent, acidic thiourea as a stripping agent, and sorbitan monooleate (Span 80) as a surfactant was attempted. A suitable range of mixed carrier concentration on the facilitated extraction performance of silver was first determined. Response surface methodology (RSM) was applied to optimize and evaluate the effect of mixed carrier concentration, stripping agent concentration, and treat ratio on the stability of the process. The results showed that the system was stable with no breakage or swelling. At the optimum condition of 8.26/12.39 mM Cyanex 302/Cyanex 272, 1.27 M acidic thiourea, and 0.62 treat ratio, the silver extraction performance and recovery were 97% and 54% (4.33 times enrichment), respectively. Further modification of the process and addition of 5% w/v of modifier resulted in 6.57 times enrichment, which accounted for 82% of the silver recovery. Hence, this study shows the capability of silver recovery using a synergistic ELM process and potential to be applied in industrial effluent.

Keywords: Emulsion Stability, Enrichment, Response Surface Methodology, Silver Recovery, Synergistic Formulation

INTRODUCTION

Silver, or Ag, is a soft, white transition metal that is ductile, malleable, and used to produce coins and jewelry. Its good heat and electrical conductivity allow the production of electronic and electrical devices. In modern times, silver has been used for catalysts and photographic film, and its anti-inflammatory and antimicrobial properties have been found useful in surgery, wound dressings, treatment of burns, and other antibiotic functions [1,2]. Silver is obtained from natural resources, mainly as a by-product of mining other metals such as gold, copper, lead, and zinc. As the natural resources of silver began diminishing, numerous researches were conducted to recover silver from secondary sources, primarily industrial wastewater. One of the potential sources is the silver electroplating process, where a significant amount of liquid waste is generated from the rinsed water of the electroplated parts. This wastewater contains an adequate amount of silver, but an appropriate treatment method is essential to recover this valuable precious metal for both environmental and economic concerns. Generally, most electroplating factories do not have any facilities for wastewater treatment.

In recent years, considerable literature has been reported on the available methods for metal recovery and wastewater treatment from electroplating industries, including chemical precipitation, coagulation and flocculation, ion exchange, membrane filtration, adsorption, electrochemical treatment, and photocatalysis [3-5]. However, silver content and concentration in the industrial effluent are extremely low (5-50 ppm) [6], which complicates the recovery process by chemical and physical methods. Therefore, more efficient techniques for the recovery process are required. One of the alternative methods to recover silver is the emulsion liquid membrane (ELM) process. This technology was developed based on the combination of membrane separation and solvent extraction into a single unit operation. The advantages of ELM include low energy requirement, fast extraction due to large mass transfer area, high efficiency, very selective to the target solute, and the potential to recover substances from dilute solutions [7,8].

Selecting the right formulation is critical for improving the selectivity of an ELM operation, but it can be time-consuming and pricey. The formulation consists of a carrier, diluent, surfactant, and stripping agent. Previously, a single carrier was used in the extraction process. Unfortunately, the application of a single carrier in the liquid membrane formulation causes small loading capacity and sluggish phase separation [9,10]. To improve the efficiency of ion transport and process, a synergistic extraction system could be developed. Synergism involves the cooperation or interaction of two or more carriers, where the combined effect is larger compared to the sum of the individual carrier effects. The synergistic extraction process can be carried out with a combination of any type of carrier. For instance, Sulaiman et al. [11] investigated the extraction of reactive dye using a synergistic mixture of Aliquat 336 and D2EHPA carriers. Another study reported a synergistic extraction system using

†To whom correspondence should be addressed.
E-mail: norasikin@cheme.utm.my

a mixture of M5640 and TRPO for the separation of copper from nickel [12]. Hu et al. [13] attempted recovery of scandium using a mixture of Cyanex 923 and Cyanex 272. The use of synergistic carriers is significant in enhancing the extraction performance as well as avoiding the time-consuming development of new carriers. Also, an appropriate formulation would be able to reduce the consumption of expensive chemicals. On the other hand, a petroleum-based diluent is commonly used in the formulation, which is non-renewable, flammable, volatile, hazardous, and not considered environmentally friendly. By replacing the diluent with renewable, safer, and nontoxic palm oil [14], facing the challenges to encourage green chemistry via the ELM process is more feasible.

The key disadvantage of the ELM process is emulsion stability, which is related to emulsion breakage and swelling. Stability of the liquid membrane is defined as its ability to resist leakage or rupture in the process of solute extraction [15]. Emulsion breakage, the rupture of the emulsion, diminishes some of the solute separations that have been achieved. As a result, the volume of the stripping phase and solute recovery are affected. Meanwhile, swelling is the incorporation of some feed phase into the emulsion. It causes the volume of the stripping phase to increase and consequently induces several related problems in the ELM process. There are several studies on factors contributing to emulsion stability that are particularly related to the emulsion formulation, processing condition, and emulsification procedure [16-18].

The success of this technology also depends on the optimization of the processing conditions. To optimize the ELM process and find the interaction between parameters, a suitable mathematical and statistical technique known as response surface methodology (RSM) can be implemented. RSM uses data from a fitted experimental design to solve the effect of parameters simultaneously. Previously, Rosly et al. [19] applied RSM to investigate the effect and optimization parameters of phenol removal in the emulsion liquid membrane process. Park et al. [20] studied experimental optimization through RSM for anionic dye removal. Another study reported optimization of propionic acid recovery from dilute aqueous solution using RSM [21]. The model equation obtained in RSM must describe the individual, interaction, and combined effects of all independent parameters.

To the best of our knowledge, no research has been reported yet concerning the optimization of synergistic green ELM stability for silver recovery. In this study, the extraction of silver was attempted using the synergistic green formulation as described by Jusoh et al. [22] containing palm oil as a diluent, Cyanex 272 and Cyanex 302 as carriers, Span 80 as a surfactant, and acidic thiourea as a stripping agent. The RSM method was employed to optimize and evaluate the effect of independent parameters on the emulsion stability. The performance of silver recovery was further evaluated at the optimum condition from the RSM study.

METHODOLOGY

1. Chemicals

Silver nitrate ($AgNO_3$) solution as feed phase and thiourea (99% purity) were purchased from Merck. Refined cooking palm oil was supplied by Lam Soon Edible Oils (Brand: Buruh). Bis (2,4,4-trimethylpentyl) phosphinic acid (Cyanex 272, 90% purity) was obtained from Fluka. Bis (2,4,4-trimethylpentyl) monothiophosphinic acid (Cyanex 302, 99% purity), sorbitan monooleate (Span 80, ≥60%oleic acid), sulfuric acid (≥95%), and octanol (99% purity) were obtained from Sigma Aldrich. All chemicals were used as produced without any additional purification step.

2. Experimental Design

Response surface methodology (RSM) was employed in the optimization of silver extraction using Statistica 8.0 (Stat Soft). An experimental design comprising three independent parameters was obtained using Box-Behnken design (BBD). The effect of mixed carrier concentration, stripping agent concentration, and treat ratio was investigated and denoted as X_1, X_2, and X_3, respectively. Accordingly, 15 experimental runs were designed to study the parameters at three levels coded as −1, 0, and +1. The data from the designed set of experiments were optimized to evaluate the individual, interaction, and combined effects between the independent parameters as well as their effects on the emulsion stability (dependent parameters). A second-order polynomial response function of emulsion stability, Y, was estimated from regression analysis as presented in Eq. (1).

$$Y = \beta_0 + \sum_{i=1}^{k} \beta_i X_i + \sum_{i=1}^{k} \beta_{ii} X_i^2 + \sum_{i=1}^{k-1} \sum_{j=2}^{k} \beta_{ij} X_i X_j \quad (1)$$

where Y is the response to be predicted, β_0 is the central point estimated coefficient, β_i, β_{ii}, and β_{ij} are the estimated coefficients from regression, which represent the linear, quadratic, and cross products of independent parameters X_1, X_2, and X_3 towards dependent parameters. Table 1 displays the range of the experiment and coded levels of independent parameters studied.

Analysis of variance (ANOVA) was employed to validate the estimated response function. Fisher's (F) test was conducted to evaluate the significance and efficacy of the fitted model. To determine the significance of the model coefficient, the student's *t*-distribution and *p*-value were analyzed. The individual, interaction, and combined effects of all independent parameters were determined from two- and three-dimensional response surface plots.

Table 1. Range of experiment and coded levels of independent parameters

Parameters	Range and levels		
	−1	0	+1
Mixed carrier concentration (mM), X_1	6.0/9.0	8.0/12.0	10.0/15.0
Stripping agent concentration (M), X_2	0.5	1.0	1.5
Treat ratio, X_3	0.20	0.33	1.00

3. ELM Procedures

An organic membrane solution (Cyanex 272, Cyanex 302, and Span 80 in palm oil) was emulsified with stripping solution (acidic thiourea solution) through a motor-driven homogenizer (Heidolph Silent Crusher M) for 5 minutes at 7,000 rpm [23]. The white milky emulsion obtained was distributed in the external feed phase and stirred using an agitator (Cole Parmer, model EW-50006-00). The extraction process was based on the aforementioned experimental design as described in Section 2 of methodology. The mixed carrier concentration, stripping agent concentration, and treat ratio were varied according to the experimental runs obtained using BBD. Other conditions, such as surfactant concentration, extraction time, agitation speed, and stripping agent to diluent ratio, were fixed at 3% w/v, 5 minutes, 300 rpm, and 1 : 3, respectively. After extraction, the external phase was separated from the emulsion phase via gravity settling in the separation funnel. A heat-induced demulsification technique was used to demulsify the emulsion into the liquid membrane and internal phase. Ultrasonic vibration (LIR biotech 020S) was used at a frequency of 40 kHz for 10 minutes to initiate the demulsification process. The emulsion was then heated at 70 °C for 24 hours [24]. An appropriate dilution was made to the internal phase collected before silver concentration determination using atomic absorption spectrometry (AAS). The performance of ELM in terms of extraction, enrichment ratio (ER), and recovery was determined using Eqs. (2) to (4). The stability of the emulsion was represented by the percentage of emulsion swelling as shown in Eq. (5).

$$\text{Extraction (\%)} = \frac{C_{i,ext} - C_{f,ext}}{C_{i,ext}} \times 100 \quad (2)$$

$$\text{Enrichment ratio (ER)} = \frac{C_{f,int}}{C_{i,ext}} \quad (3)$$

$$\text{Recovery (\%)} = \frac{C_{f,int}}{4TR \times C_{i,ext}} \times 100 \quad (4)$$

$$\text{Stability (\% swelling/breakage)} = \frac{V_{f,em} - V_{i,em}}{V_{i,em}} \times 100 \quad (5)$$

where $C_{i,ext}$, $C_{f,ext}$ and $C_{f,int}$ are the silver concentrations (ppm) in the initial external phase, final external phase, and final internal phase, respectively. Meanwhile, TR, $V_{i,em}$ and $V_{f,em}$ are treat ratio (ratio of emulsion to feed phase), initial and final volume of the emulsion, respectively.

EXTRACTION MECHANISM

The extraction chemistry of extracted solute in the ELM process is generally analogous to the liquid-liquid extraction mechanism [25]. The transport of a solute, on the other hand, is dominated by kinetic rather than equilibrium parameters. In the ELM process, the rapid extraction occurs due to the large interfacial area as well as simultaneous extraction and stripping reaction. Therefore, the equilibrium limitation can be neglected. Meanwhile, the transport of silver in the ELM is influenced by the concentration difference between the internal and external phases, where the silver ion is transferred from a higher concentration to a lower concentration region. The facilitated transport of silver by the synergistic carrier can be explained in two stages, as illustrated in Fig. 1. Silver ion (Ag^+) reacts with Cyanex 302 and Cyanex 272 to form complexes at the external interface as shown in Eq. (6) [22].

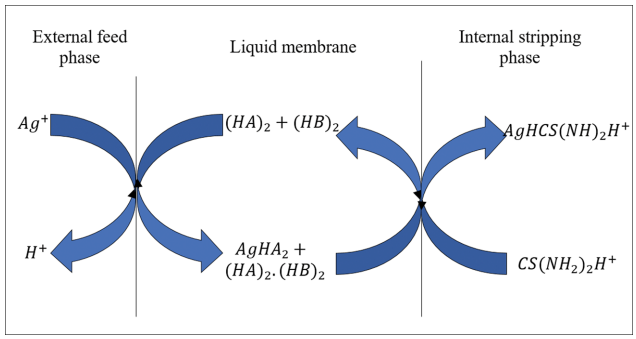

Fig. 1. Synergistic ELM transport mechanism of silver ion.

$$10Ag^+ + 20(HA)_2 + (HB)_2 \rightarrow 10(AgHA_2) + 10(HA)_2.(HB)_2 + 10H^+ \quad (6)$$

where $(HA)_2$ and $(HB)_2$ are the dimeric form of Cyanex 302 and Cyanex 272 that commonly exists in organic solvents of low polarity [26].

The complex formed ($AgHA_2$) was transported to the internal interface through the liquid membrane by diffusion. Silver from the complex was then stripped as shown in Eq. (7), releasing a free carrier that diffused back to the external interface and formed complexes with another silver ion. Other than the silver concentration difference between the internal and external phases, the transport process of silver was also influenced by the carrier that existed in the liquid membrane phase [16].

$$AgHA_2 + CS(NH_2)_2H^+ \rightarrow (HA)_2 + AgHCS(NH)_2H^+ \quad (7)$$

RESULTS AND DISCUSSION

1. Extraction

To study the performance of the ELM process on silver extraction, the effect of mixed carrier concentration was investigated.

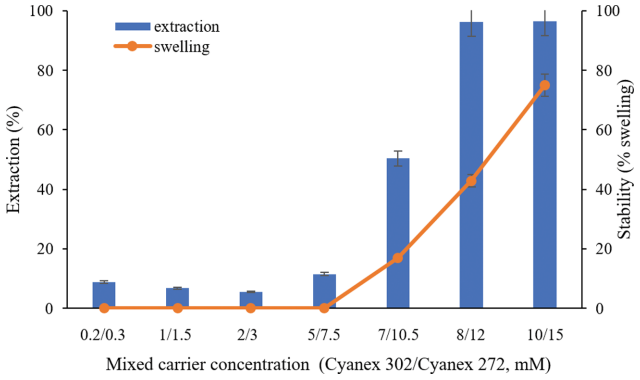

Fig. 2. Effect of carrier concentration on the extraction of silver extraction (experimental condition: feed: 50 ppm $AgNO_3$; Span 80: 3% w/v; agitation speed: 300 rpm; extraction time: 5 minutes; acidic thiourea: 1 M; treat ratio: 0.33).

Previously, a carrier mixture of 0.2 mM Cyanex 302 and 0.3 mM Cyanex 272 demonstrated synergism during the liquid-liquid extraction of 10 ppm silver [22]. Therefore, the ratio of Cyanex 302 to Cyanex 272 was maintained at 2 : 3. Fig. 2 shows the performance of silver extraction at different Cyanex 302/Cyanex 272 concentrations in the range of 0.2/0.3 mM to 10/15 mM. At low carrier concentration (0.2/0.3-5/7.5 mM), there was no significant increase in silver extraction, and around 10% of extraction was recorded. This was because the amount of carrier was insufficient to extract all the silver ions in the external feed phase. There is a clear trend of increasing extraction performance from 11.5% to 96% with carrier concentration from 5/7.5 to 8/12 mM, respectively. This result was attributed to the increment of carrier molecules to react with silver ion at a higher concentration, thus enhancing the percentage of extraction. This is supported by Kumar [17] who stated that the extraction efficiency depends on the concentration of carrier.

With an increment to the carrier concentration up to 10/15 mM, the extraction performance plateaued at 96%. However, it can be seen from the graph that there was an increment in emulsion swelling with carrier concentration because the excess carrier was added in the liquid membrane phase. Around 75% of emulsion swelling was recorded, which is very unfavorable in the ELM process. This is likely to be related to excessive carrier concentration, which resulted in higher liquid membrane viscosity as well as promoting water to be transported from the external phase. This finding is consistent with Mokhtari and Pourabdollah [27], who also found that emulsion was unstable at a higher carrier concentration during extraction of bismuth. As a result, a considerable reduction in silver concentration in the recovery phase was observed. Therefore, emulsion stability was further investigated.

2. Optimization of ELM Stability

To develop a successful ELM process with high stability, the process parameters were optimized using RSM. The effect of independent parameters, such as mixed carrier concentration (X_1), stripping agent concentration (X_2), as well as treat ratio (X_3), on the response parameter (ELM stability) was investigated. Table 2 shows the Box-Behnken design matrix along with the experimental and predicted values. Each of the parameters were expressed in coded terms to facilitate the estimation of the coefficients at three levels (−1, 0, +1).

A second-order polynomial model was obtained from the multiple regression analysis of the experimental results of ELM stability as shown in Eq. (8). The parity plot in Fig. 3 compares the predicted values of the ELM stability with the observed experimental values. The coefficient of determination (R^2) value for ELM stability was 0.98972, signifying that 98.97% of the data variability was explained in the model. Meanwhile, only 1.03% of the data variations were not accounted for in the model. Furthermore, the observed

Table 2. Box-Behnken design matrix together with the experimental and predicted values of ELM stability

Run	Coded values			Stability (% swelling)	
	X_1	X_2	X_3	Experimental	Predicted
1	−1	−1	0	30	33
2	+1	−1	0	100	101
3	−1	+1	0	70	69
4	+1	+1	0	20	17
5	−1	0	+1	100	101
6	+1	0	+1	100	104
7	−1	0	−1	50	47
8	+1	0	−1	80	78
9	0	−1	+1	100	95
10	0	+1	+1	60	60
11	0	−1	−1	20	22
12	0	+1	−1	50	53
13	0	0	0	20	23
14	0	0	0	30	23
15	0	0	0	20	23

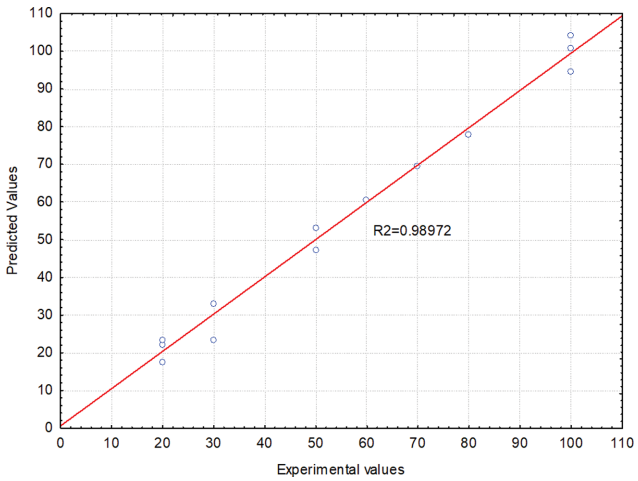

Fig. 3. Predicted versus experimental values for the ELM stability.

experimental data were fairly distributed along the 45° straight line, showing the predicted and experimental values are in good agreement. Thus, the quadratic model shown in Eq. (8) is a well-suited design of the experiment for ELM stability.

$$Y=84.1100+17.0496X_1-1.5805X_2+12.9935X_3-28.3333X_1^2-3.3333X_2^2 -52.9935X_3^2-60.0000X_1X_2+13.6319X_1X_3+32.7175X_2X_3 \quad (8)$$

The ANOVA and regression analysis for the obtained quadratic model of ELM stability is shown in Table 3. The results

Table 3. Analysis of variance (ANOVA) for the second-order model of ELM stability

Sources	Sum of square	Degree of freedom	Mean squares	F-value	F-tabulated (α=0.05)
Regression	14,977.8	9	1,664.2	53.4989	>4.77
Residual	155.54	5	31.1072	-	-
Total	15,133.33	14	-	-	-

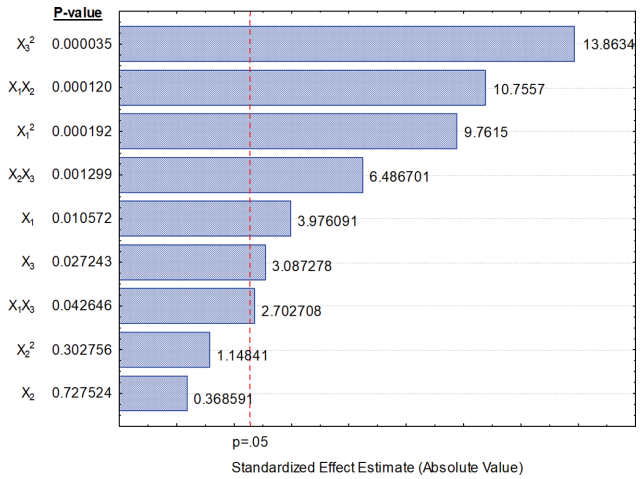

Fig. 4. Pareto chart of each parameter coefficient for ELM stability.

show that the F-value for ELM stability was 53.4989, which was greater than the tabulated F-value at 0.05 significant level ($F_{0.05,9,5}$= 4.77). The F-value calculated that was larger than F-value tabulated indicates the null hypothesis can be rejected. Note that the null hypothesis is accepted if all parameters in ELM stability give no significant effect. In this work, the parameters were significant, and the model was tested to give the prediction of a good response at a high confidence level (95%).

The Pareto chart in Fig. 4 displays the student's *t*-distribution and the corresponding *p*-value for the parameters in Eq. (8). A *p*-value of lower than 0.05 indicates the model coefficients are significant. The results of this study show that the linear model coefficients of mixed carrier concentration, X_1 (P=0.010572), and treat ratio, X_3 (P=0. 0.027243) have a significant effect on the system. Furthermore, the quadratic model terms of X_1^2 (P=0.000192) and X_3^2 (P=0.000035) also significantly affect the ELM stability. The largest effect on the stability was the quadratic coefficient of treat ratio, X_3^2 with the smallest *p*-value (0.000035) and largest *t*-value (13.8634).

Based on the quadratic model equation, a three-dimensional surface plot representing ELM stability as a function of two factors within the experimental ranges was formed as shown in Fig. 5. The circular and ellipse contour plot implied the interaction between parameters was significant and insignificant, respectively

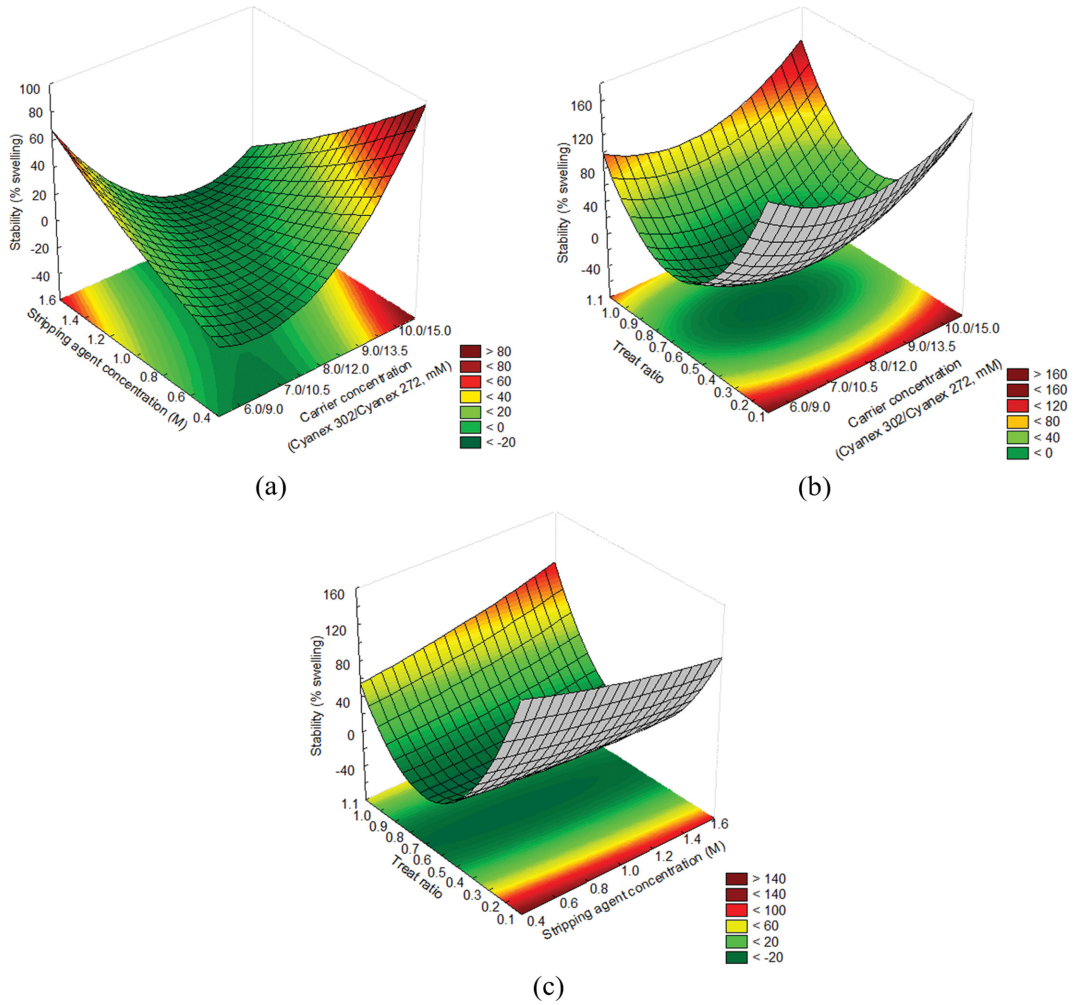

Fig. 5. The 3D surface plot of ELM stability (swelling percentage): (a) effect of stripping agent concentration and mixed carrier concentration, (b) effect of treat ratio and mixed carrier concentration, and (c) effect of treat ratio and stripping agent concentration.

[28]. Meanwhile, the critical point of the obtained quadratic model can be categorized as maximum, minimum, and saddle [19].

The interaction between the mixed carrier concentration (X_1) and stripping agent concentration (X_2) is presented in Fig. 5(a). It is apparent that the interaction between both parameters is significant owing to the elliptical nature of the contours. This can be attributed to the reaction between carrier molecules and the stripping agent that occurs at the internal interface. The highest stability (system with the lowest swelling) was indicated by the surface with the dark green color. At all ranges of striping agent concentration (0.5-1.5 M), the stability of ELM increased with mixed carrier concentration to 8.26/12.39 mM and decreased beyond the range. This is due to the higher content of the carrier, which led to a more viscous liquid membrane. Consequently, the swelling effect was diminished owing to the resistance of water molecule transport into the internal phase at higher viscosity. This finding is consistent with Sulaiman [16] who reported higher liquid membrane viscosity at higher carrier concentrations.

However, a further increase in mixed carrier concentration caused water transport phenomena to occur and led to a more serious swelling effect. This was owing to the structural features of Cyanex 302 and Cyanex 32 that are similar to the surfactant that promoted water transport at a higher concentration. For instance, a polar hydrophilic head (the phosphinate group) and a nonpolar hydrophobic tail (bis(2,4,4-trimethypentyl) groups) existed in the structure as shown in Fig. 6 [29]. The hydrophilic head promoted the water molecules to be transported into the internal phase, thus causing swelling. This finding is consistent with the work of Tang [1] who also found emulsion instability and swelling at excess carrier concentration.

Meanwhile, at a lower range of mixed carrier concentration (6.0/9.0 mM), the emulsion stability decreased with stripping agent concentration. In general, the higher the concentration of the stripping agent, the higher the transport of solute through the liquid membrane since the driving force was enhanced. Nevertheless, further increase in stripping agent concentration reduced the ELM stability as a result of greater ionic strength in the internal phase. Thus, the emulsion swelled osmotically. This result broadly supports the work of previous research by Goyal et al. [30]. In contrast, the emulsion stability increased with stripping agent concentration at a high range of mixed carrier concentration (10.0/15.0 M). This is due to increased stripping agent capacity to react with the solute-carrier complex, thus reducing the swelling effect from the excess carrier.

Fig. 5(b) demonstrates the interaction between mixed carrier concentration (X_1) and treat ratio (emulsion to external feed phase, X_3). The elliptical contour plot indicates the interaction between these parameters was significant. The best condition for the most stable emulsion was shown by the green confined surface and smallest curve in the plot. For all treat ratio ranges (0.2-1.0), the stability of the emulsion enhanced with carrier concentration up to 8.26/12.39 mM, owing to the suitable viscosity condition for a stable liquid membrane layer. The emulsion stability reduced with a further increment in carrier concentration due to the excess amount of carrier creating an affinity for water molecules to be transported into the internal phase and inducing swelling. For all mixed carrier concentration ranges (6.0/9.0-10.0/15.0 mM), the stability of the emulsion improved with a treat ratio up to 0.62 and declined afterward. This was because the emulsion mass transfer area and the external phase volume were controlled by the treat ratio. It can be seen at a treat ratio of 0.2 that the emulsion was unstable. Theoretically, the emulsion can be properly dispersed in a larger volume of external phase, producing a high number of emulsion globules and resulting in a larger mass transfer area [31]. Unfortunately, this condition leads to emulsion breakage owing to the continuous transportation of water molecules into the internal phase due to surfactant hydrolysis. With an increment to the treat ratio up to 0.62, the emulsion swelling was reduced, indicating that the ELM system was stable at this condition. Meanwhile, the emulsion was unstable when the treat ratio was raised to 1.0. In a smaller external phase volume, the emulsion could not be well dispersed and larger emulsion globules were formed. In the meantime, co-transport of water by surfactant occurred, which resulted in emulsion instability and internal phase dilution.

The interaction between stripping agent concentration (X_2) and treat ratio (X_3) is shown in Fig. 5(c). The ellipse contour implies the interaction of these parameters was significant. For all stripping agent concentration ranges (0.5-1.5 M), the emulsion stability enhanced with a treat ratio up to 0.62 and became unstable afterward. A possible explanation for this is the osmotic pressure between the external phase and emulsion was reduced at a higher treat ratio, which resulted in better emulsion stability. However, an increment to the treat ratio to 1.0 diminished the emulsion stability. This was owing to the larger formation of emulsion globules as well as the co-transport of water molecules into the internal phase. Meanwhile, a lower significant effect on emulsion stability was observed with the concentration of stripping agent for all treat ratio ranges (0.2-1.0). This finding is likely to be related to the osmotic swelling of the system that is controlled by the treat ratio. This pattern indicates that the treat ratio has a greater impact than the concentration of stripping agent, which was in line with the data presented in the Pareto chart (Fig. 4).

From the optimization study, the critical point for the second-order model presented in Eq. (8) and the response surface plot can be determined. The optimum condition parameter for ELM stability obtained was a minimum point at 8.26/12.39 mM carrier

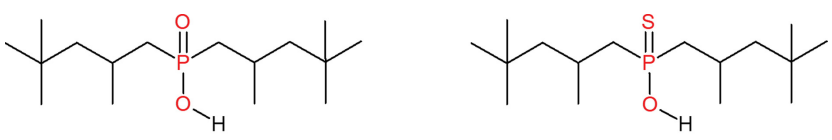

(a) (b)

Fig. 6. Chemical structure of (a) Cyanex 272 and (b) Cyanex 302.

Table 4. Validation of optimized data for ELM stability

Optimum parameters	RSM predicted	RSM observed	
	Stability (%)	Stability (%)	Enrichment
Mixed carrier concentration: 8.26/12.39 mM Stripping agent concentration: 1.27 M Treat ratio: 0.62	−25.83	0	4.33

concentration, 1.27 M stripping agent, and 0.62 treat ratio. At the predicted optimum condition, the predicted stable emulsion was -25.83%, indicating no swelling effect. To validate the prediction, the emulsion stability was observed at the optimized condition and the results found that 0% of stability was achieved. This indicates that the observed experimental results were in parallel with the values predicted from the RSM study. The finding also implied that RSM is applicable for use in the optimization of ELM stability. On the other hand, the enrichment of silver in the internal phase was around 4.33, which represented 54% recovery. The verification of optimized data for stability is summarized in Table 4.

3. Prospect of the Recovery Process

Separation of silver in terms of extraction and recovery is critical in the ELM process. The aforementioned results show that the ELM was stable with 96% of extraction and 4.33 times enrichment (54% recovery) as shown in Fig. 7. To improve silver recovery while enhancing or maintaining the stability of the emulsion, further modification to the system was investigated. Previously, the addition of modifiers had been investigated by some researchers [32,33]. The presence of modifiers in the liquid membrane reportedly improved the structure of the emulsion, which resulted in better extraction and recovery. Since Cyanex 302, Cyanex 272, and palm oil used in this work is very viscous [34], components such as alcohol are required to modify the liquid membrane properties. This is due to alcohol which solubilizes in the tail region of the surfactant and forms reverse micelles reported to increase the rigidity of the interface [35].

The results indicated that the addition of 5% (w/v) octanol slightly increased the enrichment of silver in the internal phase to 4.52 times (57% recovery) and the system was stable during the process. The increase in the recovery is due to the improved solubility of the permeated carrier-solute complex that is transported in the liquid membrane phase. This result further supports the idea of El-Nadi [36] who stated poor solubility of the extracted species would result in the formation of the third phase between the diluent and the aqueous phases. To inhibit this third phase formation, a modifier is usually added to the diluent in order to increase the solubility of the extracted species. Nevertheless, when the modifier concentration was raised up to 10% in the liquid membrane phase, a significant reduction of silver recovery was observed to 3% (0.24 enrichment). In addition, the system was unstable with 40% of breakage recorded. This result is likely to be related to the excess octanol producing unfavorable emulsion with less viscosity, which tends to rupture when exposed to shear provided by the impeller during the ELM process. These results agreed with other studies relating emulsion instability with low emulsion viscosity [37]. Consequently, the modifier concentration was fixed at 5% (v/v) to maximize the silver recovery percentage.

It was demonstrated the modification could retain the stability and increase the enrichment of silver in the internal phase. Theoretically, the enrichment should reach around 8 for maximum recovery using this formulation. This is based on the volume ratio of silver in the external phase that will be confined in the internal phase. A possible explanation for this is that the small scale of emulsion volume used during the process was not suitable for demulsification. To improve the process, further modification was

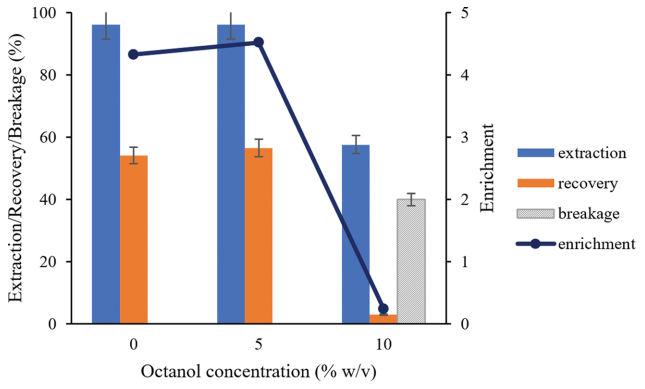

Fig. 7. Effect of modifier concentration (octanol) on enrichment of silver (experimental condition: feed: 50 ppm $AgNO_3$; carrier concentration: 8.26/12.39 mM Cyanex 302/Cyanex 272; Span 80: 3% w/v; agitation speed: 300 rpm; extraction time: 5 minutes; thiourea: 0.1 M; H_2SO_4: 1.27 M; treat ratio: 0.62).

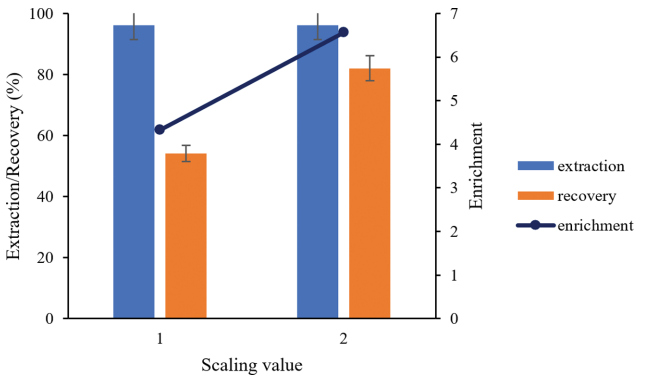

Fig. 8. Effect of scaling volume on the ELM process of silver. (experimental condition: feed: 50 ppm $AgNO_3$; carrier concentration: 8.26/12.39 mM Cyanex 302/Cyanex 272; Span 80: 3% w/v; agitation speed: 300 rpm; extraction time: 5 minutes; thiourea: 0.1 M; H_2SO_4: 1.27 M; treat ratio: 0.62; Octanol concentration: 5% w/v).

conducted by scaling the emulsion and external phase volume to 200% as shown in Fig. 8.

The result shows 6.57 times of silver was concentrated in the internal phase which is equivalent to 82% recovery. This result can be explained by the fact that higher volume could occupy considerable energy provided from the impeller. Therefore, the emulsion could be dispersed properly and the emulsion globule and droplet size are much smaller and provide adequate stability for the extraction and recovery processes [38]. This indicates that a smaller size of droplets and globules will increase the mass transfer due to a larger interfacial area and possible active sites on the membrane phase that are available for the extraction and recovery processes. The diffusional path inside the emulsion globules also became shorter as the size of the emulsion became smaller. Subsequently, the free carrier could be released faster in the confined internal phase and circulated again to the external interface, and react with another silver ion. Therefore, the carrier-silver complex accumulation in the liquid membrane phase can be prevented. This study produced results that corroborate the findings of Ammar et al. [39].

CONCLUSION

The feasibility of the stability optimization of the synergistic green ELM process for the recovery of silver from an aqueous solution was demonstrated. At the optimum condition of 8.26 mM Cyanex 302, 12.39 mM Cyanex 272, 1.27 M acidic thiourea, 0.62 treat ratio, the system was stable with no breakage or swelling. Meanwhile, the extraction and recovery of silver was 97% and 54% (4.33 times enrichment), respectively. Further modification on the process and addition of 5% w/v of modifier resulted in 6.57 times enrichment, which accounted for 82% of the silver recovery. Therefore, the finding of this study shows the potential to expand the research on the industrial effluent treatment process.

ACKNOWLEDGEMENTS

The authors are grateful to the Ministry of Higher Education (MOHE), Universiti Teknologi Malaysia (Research Grant; PDRU: Q.J130000.21A2.04E65, Q.J130000.21A2.05E51, CRG 40.0: Q.J130000.2451.08G02, and CRG 40.3: R.J130000.7309.4B413), and Centre of Lipids Engineering and Applied Research, Ibnu Sina Institute for Scientific and Industrial Research for providing the financial support and facilities to perform the research work.

REFERENCES

1. B. Tang, G. Yu, J. Fang and T. Shi, *J. Hazard. Mater.*, **177**, 377 (2010).
2. C. Jeon, *Korean J. Chem. Eng.*, **34**, 384 (2017).
3. C. Liu, N. Fiol, J. Poch and I. Villaescusa, *J. Water Process Eng.*, **11**, 143 (2016).
4. T. Scarazzato, Z. Panossian, J. A. S. Tenório, V. Pérez-Herranz and D. C. R. Espinosa, *J. Cleaner Prod.*, **168**, 1590 (2017).
5. M. Kobya, E. Demirbas, F. Ozyonar, G. Sirtbas and E. Gengec, *Process Saf. Environ. Prot.*, **105**, 373 (2017).
6. B. Gielen, Silver plating industry effluent, https://www.finishing.com/433/21.shtml (2006).
7. M. Mesli and N. E. Belkhouche, *Chem. Eng. Res. Des.*, **129**, 160 (2018).
8. S. Gupta, P. B. Khandale and M. Chakraborty, *J. Dispersion Sci. Technol.*, **41**, 393 (2020).
9. M. Wu, H. He, F. Xu, Z. Xu, W. Zhang, Z. He, J. Qu, R. Chi and L. Huang, *Sep. Purif. Technol.*, **212**, 255 (2019).
10. A. S. Guimarães, L. A. Silva, A. M. Pereira, J. C. G. Correia and M. B. Mansur, *Sep. Purif. Technol.*, **239**, 116570 (2020).
11. R. N. R. Sulaiman, H. A. Rahman, N. Othman, M. B. Rosly, N. Jusoh and N. F. M. Noah, *Korean J. Chem. Eng.*, **37**, 141 (2020).
12. H. Duan, S. Wang, X. Yang, X. Yuan, Q. Zhang, Z. Huang and H. Guo, *Chem. Eng. Res. Des.*, **117**, 460 (2017).
13. J. Hu, D. Zou, J. Chen and D. Li, *Sep. Purif. Technol.*, **233**, 115977 (2020).
14. S. H. Chang, *Desalin. Water Treat.*, **52**, 88 (2014).
15. F. Moyo and R. Tandlich, *J. Biorem. Biodegrad.*, **5**, 228 (2014).
16. R. N. R. Sulaiman, N. Othman and N. A. S. Amin, *J. Ind. Eng. Chem.*, **20**, 3243 (2014).
17. A. Kumar, A. Thakur and P. S. Panesar, *Rev. Environ. Sci. Biotechnol.*, **18**, 153 (2019).
18. M. Keyvani, L. Davarpanah and F. Vahabzadeh, *Korean J. Chem. Eng.*, **31**, 1681 (2014).
19. M. B. Rosly, N. Jusoh, N. Othman, H. A. Rahman, N. F. M. Noah and R. N. R. Sulaiman, *Chem. Eng. Res. Des.*, **145**, 268 (2019).
20. H. N. Park, C. W. Cho, H. A. Choi and S. W. Won, *Korean J. Chem. Eng.*, **34**, 2519 (2017).
21. V. Inyang and D. Lokhat, *Sep. Sci. Technol.*, 1 (2021).
22. N. Jusoh, N. Othman, R. N. R. Sulaiman, N. F. M. Noah and K. S. N. Kamarudin, *J. Membr. Sci. Res.*, **7**, 59 (2021).
23. N. Jusoh, R. N. R. Sulaiman, N. Othman, N. F. M. Noah, M. B. Rosly and H. A. Rahman, *Food Bioprod. Process.*, **119**, 161 (2020).
24. W. Peng, H. Jiao, H. Shi and C. Xu, *Desalination*, **286**, 372 (2012).
25. R. A. Kumbasar, *J. Ind. Eng. Chem.*, **18**, 145 (2012).
26. Z. T. Ichlas and D. C. Ibana, *Int. J. Miner. Metall. Mater.*, **24**, 37 (2017).
27. B. Mokhtari and K. Pourabdollah, *Chin. J. Chem. Eng.*, **23**, 64 (2015).
28. N. Benyahia, N. Belkhouche and J. A. Jönsson, *J. Environ. Chem. Eng.*, **2**, 1756 (2014).
29. S. Olushola, A. Folahan, A. Alafara, J. Bhekumusa and S. Olalekan, *Int. J. Phy. Sci.*, **8**, 89 (2013).
30. R. K. Goyal, N. S. Jayakumar and M. A. Hashim, *J. Hazard. Mater.*, **195**, 383 (2011).
31. H. R. Mortaheb, M. H. Amini, F. Sadeghian, B. Mokhtarani and H. Daneshyar, *J. Hazard. Mater.*, **160**, 582 (2008).
32. F. d. M. Fábrega and M. B. Mansur, *Hydrometallurgy*, **87**, 83 (2007).
33. K. Abbassian and A. Kargari, *J. Environ. Chem. Eng.*, **4**, 3926 (2016).
34. T. H. Nguyen and N. V. N. Hoa, *Metals*, **10**, 1 (2020).
35. Z. Y. Ooi, N. Harruddin and N. Othman, *Biotechnol. Progr.*, **31**, 1305 (2015).
36. Y. A. El-Nadi, *Int. J. Miner. Process.*, **82**, 14 (2007).
37. A. Kumar, A. Thakur and P. S. Panesar, *J. Ind. Eng. Chem.*, **70**, 394 (2019).
38. S. Gaikwad and A. Pandit, *Ultrason. Sonochem.*, **15**, 554 (2008).
39. S. H. Ammar, H. G. Attia and A. K. D. Affat, *FCNES*, 1 (2012).